APPLICATION OF ELECTRICAL POTENTIAL METHOD TO COMPACT TENSION SPECIMEN

by

Ferruh Gençer

Submitted to the Faculty of the Engineering
In Partial Fulfillment of the Requirements
for the Degree of

MASTER OF SCIENCE
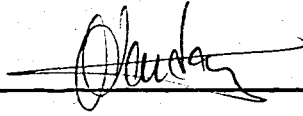in
MECHANICAL ENGINEERING
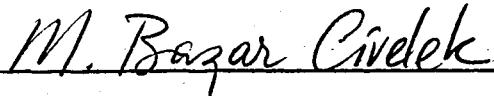
Boğaziçi University
September, 1981

APPROVED BY:

Doç.Dr.Öktem VARDAR
(Thesis advisor)

Yük.Müh.Hamit OSSA

Doç.Dr.Başar CİVELEK

ABSTRACT

In this thesis "Electrical Potential Method" is consi-
dered. It is an experimental method to monitor sub-critical
crack growth. Optimum locations for current and voltage leads
and the calibration curve for compact tension specimen have
been found using paper analogs. These results have been
verified through metallic specimens. Sharp fatigue cracks are
introduced in compact tension specimens and total crack lengths
of these specimens have been estimated my means of the
electrical potential technique. Real crack lengths are
measured through a pocket comparator after heat tinting and
separating the specimens into two. Results have been
compared and discussed.

ÖZET

Bu çalışmada, kritik-altı çatlak uzunluğu gözlemede kullanılan deneysel bir yöntem olan "Elektrik Gerilim Yöntemi" incelenmiştir. Kağıt modeller kullanılarak akım ve voltaj telleri için optimum konumlar bulunmuş, ufak çekme nümunesi için kalibrasyon eğrisi çizilmiştir. Sonuç, madenî nümunelerde yapılan ölçümlerle doğrulanmıştır. Ufak çekme nümuneleri üzerinde yorulma çatlağı başlatmak için deneyler yapılmış ve çatlak uzunlukları, elektrik gerilimi yöntemiyle ve ısıl dağlama ve kırılmadan sonra, kırılma yüzeylerinin büyütülmüş fotoğrafları üzerinde bir cep komparatörüyle ölçülmüştür. Sonuçlar karşılaştırılmış ve irdelenmiştir.

ACKNOWLEDGEMENTS

TABLE OF CONTENTS

LIST OF FIGURES

LIST OF TABLES

LIST OF SYMBOLS

a	crack length
A	area
B	thickness of specimen
c	distance measured from neutral axis to the most remote fiber of a beam
H	height
i	electrical current
I	moment of inertia
L	length
M	bending moment
N_i	number of cycles for fatigue crack initiation
P	load
R	electrical resistance
V	voltage
V_a	voltage across the crack
W	width of specimen
x	Cartesian coordinate
ρ	crack tip radius
ρ_e	electrical resistivity
σ	stress

CHAPTER I. INTRODUCTION

The sudden fracture of large structures (e.g. ships, bridges) as well as rotating machine parts, pressure vessels etc. which sometimes caused large damage led people to research, test and study on fatigue and fracture. Although one does not know all the physical facts taking place in a fracture process considerable development have been made within last 25 years on the subject. This in turn made people think of new methods of testing since the standard unnotched tensile test is not sufficient to supply us with appropriate information.

One of the most important parameters concerned is the crack length. Whether the test is on fracture mechanics or fatigue accurate measurement of the crack length at any moment of the test is essential. There are quite a number of methods developed to monitor slow-moving cracks, such as surface measurement techniques, optical, continuity gage, eddy current methods, displacement gages, ultrasonics, electrical potential method.

Electrical potential method, which is the subject of

this thesis, is found to be the most suitable because of its adaptability to standard test specimens, applicability in various temperatures (from $\sim -100^{\circ}C$ to $\sim 100^{\circ}C$) and environmental conditions, continuity - provided that the test set up has an automatic recorder-, and relatively lower cost|1|.

CHAPTER 2. ELECTRICAL POTENTIAL METHOD

2.1. REVIEW of EXISTING WORK

Electrical potential method was first employed over 30 years ago for detecting surface cracks in large scale structures. In later years it has been successfully applied to following areas |2|.

- propagation of fatigue

- hydrogen embrittlement

- stress corrosion

- creep cracks

- crack extension in COD test

- J_{IC} tests.

The method is based on the following principle:

If a current carrying body contains a discontinuity its potential field will be disturbed. If the discontinuity is a crack, the potential difference across the crack will increase as the crack extends, provided the input current is held constant.

Trost |3|, 1944, was the first to report on crack

detection by electrical potential method. He used it to detect
surface cracks in metals. Next, Gille|4|, 1956, applied this
technique to large scale structures using currents of the
order of 1000-1500 A.

The method was first employed in fracture research
studies by Barnett and Troiano|5|, 1957, who investigated
hydrogen embrittlement in circumferencially notched tensile
specimens. They used precision double Kelvin bridge to
measure the change in resistance with crack length. They
found out that increase in resistance was due to deformation
or crack advance, but in case of constant load the effect of
deformation would be negligible. Steigerwald and Hanna|6|
using again double Kelvin bridge for resistance measurement
showed that the effect of elastic deformation for rising load
tests cannot be neglected and therefore they only considered
irreversible resistance changes.

To detect the crack lengths accurately the testpiece
has to be calibrated precisely. This gave rise to studies
attempting to derive theoretical calibrations by solving
Laplace's equation as well as experimental studies. Johnson|7|
gave a relation for the uniform current situation in centre-
cracked plate with a razor slit starter notch. He based his
study on experimental results of Anctil et al|8|. A modifica-
tion of Johnson's relation was made by Che-Yu Li and Wei|9|
to give better agreement with experimental results. They used

an elliptical starter notch instead of a razor slit.

Gilbey and Pearson's|10| analytical solutions for
Laplace's equation for the potential distribution in a
homogeneous strip of metal containing a transverse crack
enabled calibration curves for simple centre and edge-cracked
specimen geometries to be developed.

For more complicated geometries, such as the ones used
in fracture testing, since analytical solutions cannot be
found directly either experimental or numerical methods are
used. Experimental calibrations have been obtained by McIntyre
and Priest|11| for the point application of current and by
Ritchie|1,2| for the case of uniform current.

Clark and Knott|12| used the conformal mapping techni-
ques in determining calibrations for cracks growing from
notches of various geometries. Also the sensitivity of the
system to the positioning of potential probes has been
determined.

With the rapid development of electronics new measuring
circuits have been designed and used in analog studies. Müllner
et al|13| determined the most favorable arrangement of measur-
ing points on paper models using a special electronic measur-
ing set-up. Hagedorn et al|14| improved this set-up by
substituting the digital voltmeter by operational amplifier
and adding a low pass filter.

Marandet et al|15| used an AC differential micro ohmmeter designed to detect the initiation and growth of crack in a steel specimen to avoid the problems associated with the use of DC.

Recent studies utilize the finite element analysis. Ritchie and Bathe|16| used finite element analysis procedure to provide theoretical calibration curves for single edge notch and compact tension fracture specimens. Aronson and Ritchie|17| solved Laplace's equation by finite element analysis to optimize the efficiency of the electrical potential method for monitoring the initiation and slow growth of cracks as applied to the compact tension fracture specimen.

This study concerns with the application of the electrical potential method to compact tension specimen (Fig. 1.1.) to monitor propagation of sub-critical crack growth.

2.2. COMPACT TENSION SPECIMEN

The compact tension specimen (CT) is single-edge notched and pin loaded in tension. It has been assumed to be one of the standard specimens for "Standard Test Method for Plane-Strain Fracture Toughness of Metallic Materials" after ASTM Designation: E 399-74|18|, the other being the bend specimen which is a single-edge notched beam loaded by three-point bending.
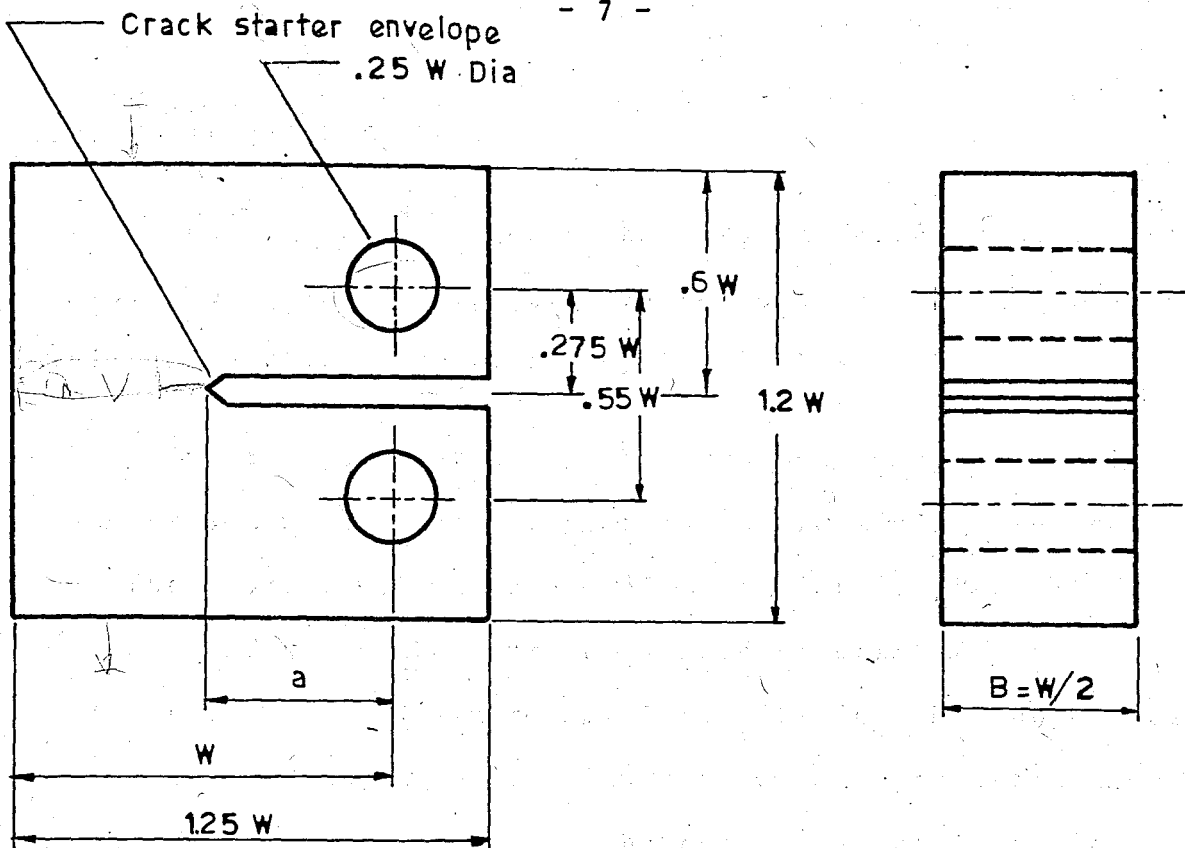
Fig. 1.1- Compact Tension Specimen

The compact tension specimen requires the least amount of material and is relatively inexpensive to test. The bend specimen requires somewhat more material but may be slightly cheaper to machine and test. Both specimens must be fatigue precracked. The compact tension must be precracked in tension-tension fatigue|19|.

The compact tension specimen is not only a standard configuration for toughness testing but also a common specimen for fatigue crack growth experiments. The requirement that the thickness (B) should be half of the specimen width (W/2) is relaxed in fatigue tests, however. Usually quite wide specimens (compared to the thickness) are utilized to obtain large amounts propagation data.

2.3. CALIBRATION CURVE

Voltage is expressed as the product of current i and resistance R, where R is given in terms of electrical resistivity ρ_e, length L and area A by $R = \rho_e L/A$.

In fracture testing as the crack extends the remaining ligament W-a will decrease, that is the remaining area conducting the current will decrease. Thus resistance R will increase and since the current is held constant the voltage across the crack will increase. By monitoring this potential difference and comparing it with a reference potential the crack length (a) or crack length-to-specimen width ratio (a/W) can be determined with the use of suitable calibration curves (Fig. 2.1.).
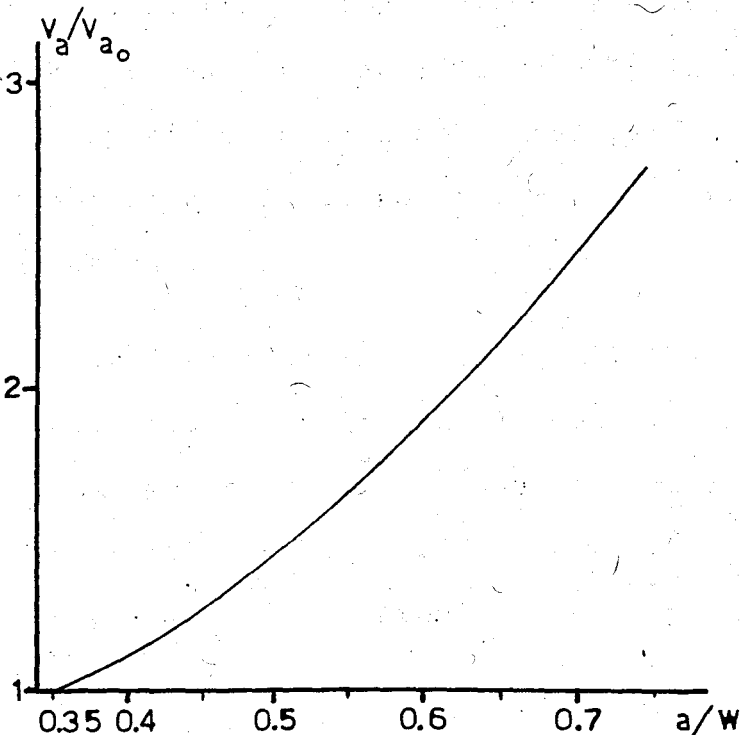

Fig. 2.1- A Typical Calibration Curve

Potential difference is a function of the specimen geometry, crack size and location of current and potential leads. But a calibration curve of non-dimensionalized type will be independent of material and specimen size, provided that all specimen dimensions are changed in proportion, including the locations of the current and voltage leads.

For accurate measurement of crack lengths precise calibration of the specimens used is inevitable. In order to satisfy this need several methods have been proposed. One of them is the analytical method which involves finding solutions to Laplace's equation for a given geometry. The steady state electrical potential is given by

$$\nabla^2 V = 0$$

for a strip of metal containing a transverse crack and of constant thickness, and current i flows only in the plane of the strip. For specimens with complicated geometry analytical solutions cannot be obtained, so either a numerical solution or an analog method is used.

If the specimen contains a crack all through the thickness graphitized electrical analog paper can be used to obtain the calibration curves. Making a pattern of the geometry in question and testing it for different crack lengths, calibration curve for that particular geometry can be easily obtained.

In this study instead of cutting the same paper to represent the crack advance, different analogs have been held ready, because an optimization analysis of current leads was also necessary. a/W ratio started with 0.35 went up to 0.75 with an increment of 0.05.

2.3.1. Apparatus

Because of the high resistivity of paper made patterns a constant current source with outputs of the order of 10^2 - 10^3 μA was necessary, such that a voltage output of 1-3 Volts could be read. A 5V DC power supply has been designed for a voltage-to-current converter circuit (Fig. 2.2. a and b).
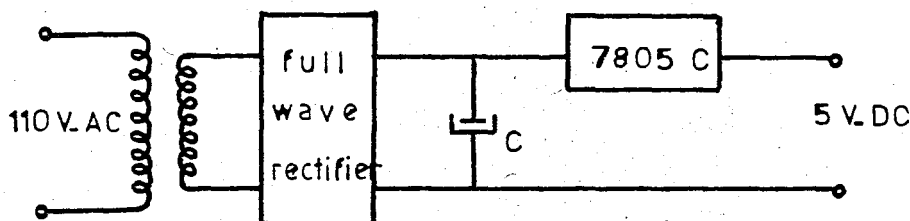
a) 5 V DC power supply
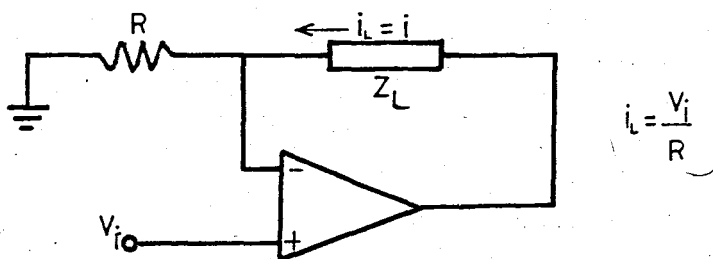
b) Voltage-to-current converter

$i_L = \dfrac{V_i}{R}$

Fig. 2.2-   Electronic circuits used in supplying constant current.

To measure the voltage output a DC multimeter   LEVELL
Type TM 9 BP has been employed. The paper patterns are placed
on a sheet of plexiglass. Both current and potential leads
were made of silver covered phosphor-bronze sheet to maximize
the conductivity. The cables connecting the contacts to
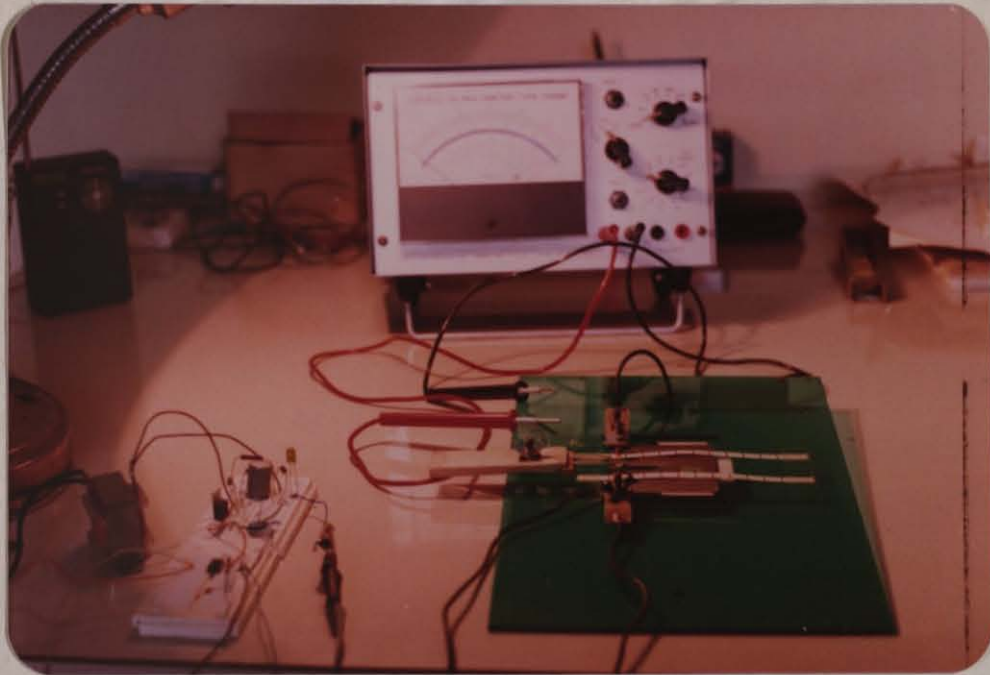corresponding instruments were copper wires (Fig. 2.3.).

Fig. 2.3- A photo of the experimental set-up

2.4. OPTIMIZATION ANALYSIS FOR CURRENT AND VOLTAGE LEAD
   POSITIONS

As in calibration curves, optimization of current and
voltage lead positions is subject to numerical (Finite Element
Analysis) or analog studies. In analog studies either electri-
cal analog paper or thin aluminium foil is being used. In

this study graphitized electrical analog paper has been preferred for both economic reasons and availability.

Before starting the optimization analysis some assumptions based on previous studies have been made. These are:

(a) Location of potential leads: A thorough analysis of papers written on the subject shows clearly that the preferred region is on top surface and as close to the notch as possible, expressed numerically within 4 mm of the notch centerline for a CT test piece with $H/W = 0,60$ and $W = 50$ mm. Here maximum reproducibility as well as maximum proportional increase in voltage (V_a/V_{a_o}) are obtained.

(b) Location of current leads: There are mainly two proposed locations. One on top surface (referred to as the standard configuration [17]), the other one on side flanks where both are point applications (Fig. 2.4).

Standard configuration which involved also location of potential leads on the same side of the specimen was previously accepted as the optimum location (actually exact positioning of the current leads is 7.5 mm from the side edge). Some numerical studies [17] on the other location show that this configuration of lead placement is superior to the standard on

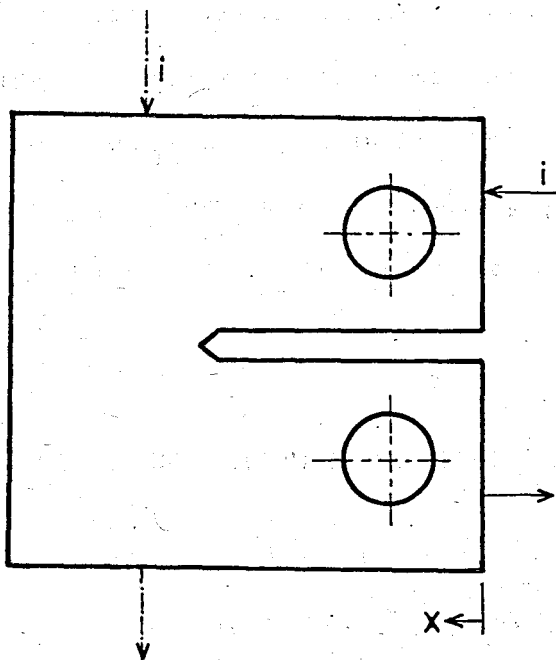Fig. 2.4- Two proposed locations for current leads in point
applications

Basically this superiority is due to reproducibility and maxi-
mization of V_a/V_{a_o} ratio. One thing remained to be still
questionable, namely "measurability". But this could be
avoided using appropriate apparatus. So, only the second case
has been investigated and optimum locations and calibration
curve for this configuration has been found.

2.4.1. Procedure

With the apparatus given above paper patterns with the smallest a/W ratio have been placed on the plexiglass sheet and starting with x = 0.5 cm (See Fig. 2.4) current location is changed by 0.5 cm each time and corresponding voltage is recorded. Once a paper model is measured completely the next one has been placed and the same process repeated. The results thus obtained are plotted in two different ways (Fig. 2.5 a and b).

2.5. CALIBRATION CURVE FOR COMPACT TENSION SPECIMEN

To obtain the calibration curve selection of optimum locations for lead placement has to be based on some predetermined criteria, namely (after Ritchie[17]):

(1) accuracy of calibration curve: The obtained curves have to be compatible with those obtained before theoretically and experimentally.

(2) sensitivity: The slope of the calibration curve has to be maximized, i.e. dV/da. So even incremental propagations of crack size can be detected.

(3) measurability: The maximization of the voltage signal $|V_a|$. Although this does not sound important when working with paper analogs, in metallic specimens due to very low resistivity it is an important factor.
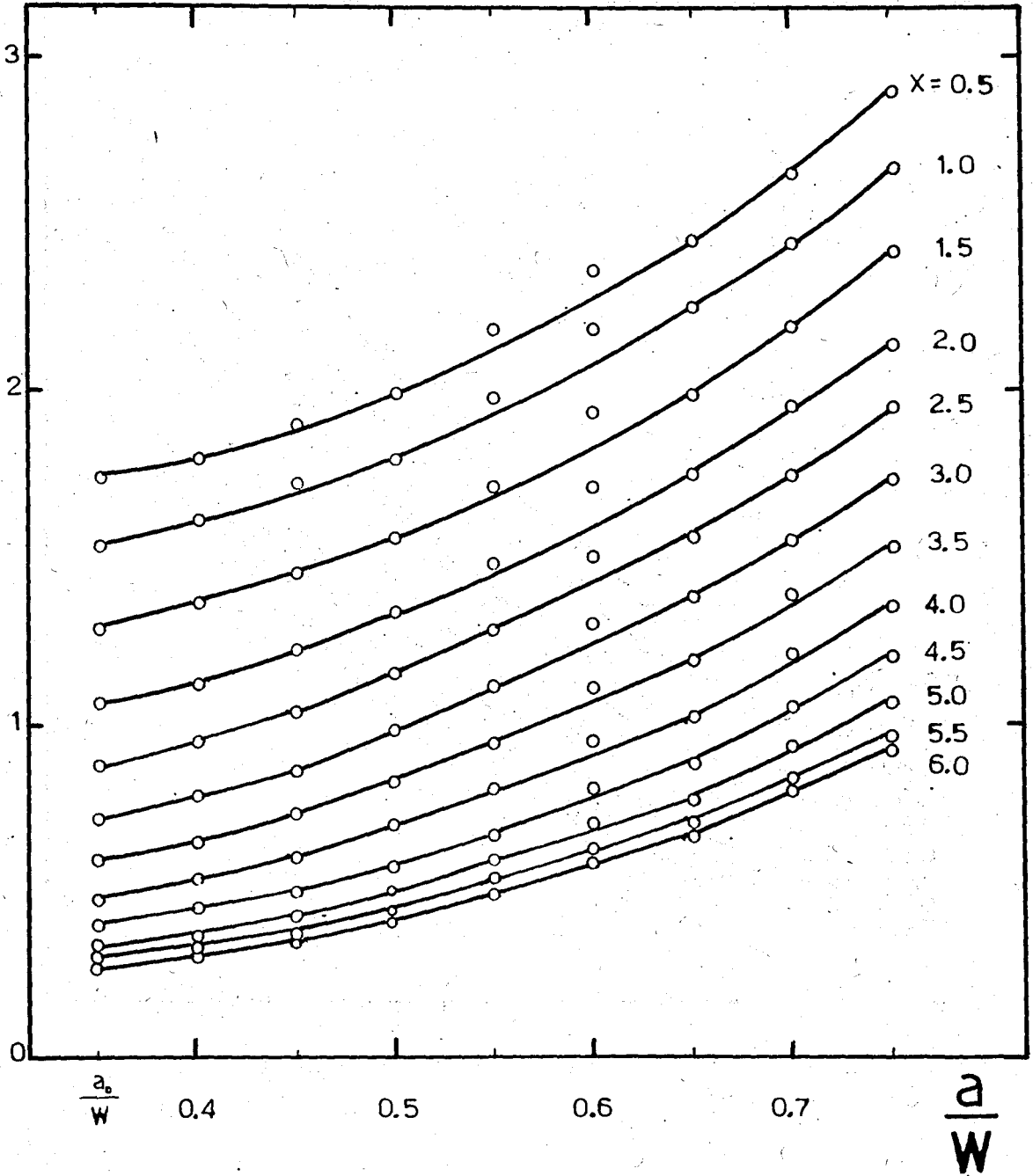
Fig. 2.5- a) Potential drop across crack vs. crack length-to-specimen width ratio
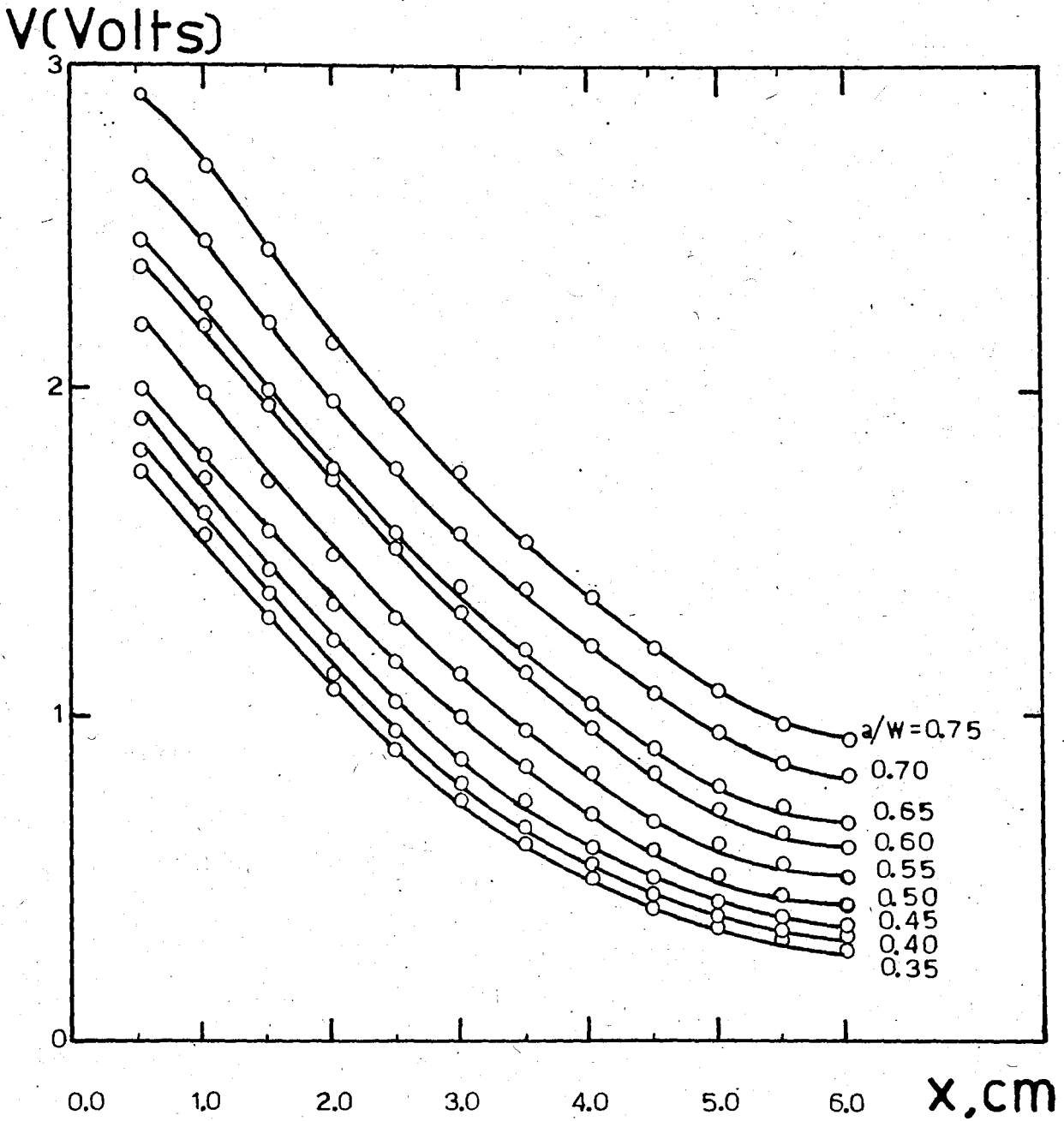
Fig. 2.5- b) Potential drop across crack vs. displacement of
current contacts along side flanks

From Fig. 2.5. a and b the best location for the current leads seems to be x = 2.5 cm, it should be added that x = 3.0 cm is also a good solution.

Plotting the calibration curve with non-dimensionaliz-ed voltages* (V_a/V_{a_0}) vs. crack length-to-specimen width ratio (a/W) and comparing it with the ones given in literature show a good fit. Also a comparison of this type of lead placement with the standard configuration shows the superiority of the former (Fig. 2.6).

Since the non-dimensionalized calibration curves should be independent of material and specimen size the next step of the study, namely proceeding with metallic specimens should yield the same curve for the same location of potential and current leads.

2.6. METALLIC SPECIMEN

Before going on with testing on a closed loop, servo hydraulic testing system (MTS 812) metallic specimens have been prepared to check the results obtained with paper models.

Here due to low resistivity of metals in general, a completely new current source have been used. Same voltmeter gave satisfactory results.

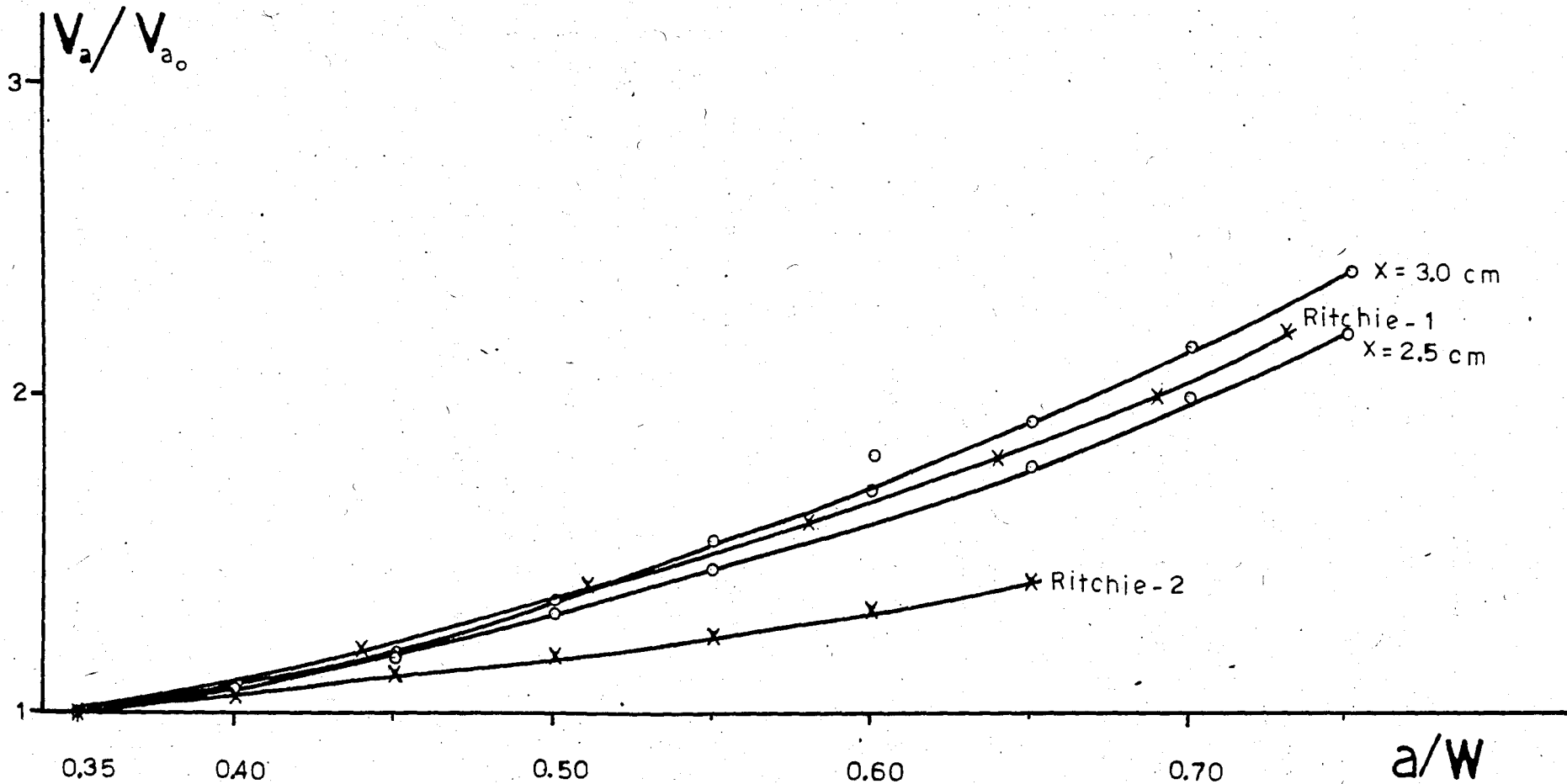* monitored voltage divided by a reference potential, here voltage of the uncracked specimen (a/W = 0.35)

Fig. 2.6- Calibration curves obtained in this study for x=2.5 and x=3.0 cm compared with
(i) Ritchie 1 - Calibration curve for configuration of current leads placed on
the midpoint of side edges|17|
(ii) Ritchie 2 - Calibration curve for standard configuration|16|

First, 7 specimens with a/W ratios 0.35, 0.39, 0.45, 0.50, 0.60, 0.66 have been machined. Material was ST 60 C-steel.

The envelope type for crack-starter notch has been chosen to be the keyhole (Fig. 2.7) because of the limitations of the machine shop and to ensure uniformity among the specimens. The thickness of all specimens was 10 mm.
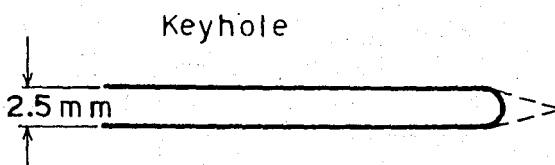
Fig. 2.7- Envelope for crack starter notch.

2.6.1. Apparatus and Procedure

A rough calculation* of the resistance of the remaining ligament indicates that quite high currents are necessary, i.e. of the order of 10 A to have voltage outputs of approximately 10^2-10^3 μV. This immediately makes one think of heating of specimen. But this is not as dangerous as it seems since the resistivity of metallic specimens is very low, such that the heat generated is negligible.

The constant current supply employed was a DC Power Supply LVR Series Model 6264 B - Hewlett Packard Its output when used as current source varies between 0-20 Amperes.

*Resistance R, given by $R = \rho_e \frac{L}{A}$ where L = 57 mm

A = (31mm) X (10mm)

ρ_e = 17.1x10^{-6} ohm-cm

the resultant resistance R≈3x10^{-5} ohm.

The next step was attaching the leads. Two proposed methods for this are spot welding and screwing. In this study screwing has been preferred.

Two holes for voltage output drilled offset diagonally across the notch to average out the effect of non-uniform crack fronts (Fig. 2.8) within $\sim$ 4 mm of notch centerline.
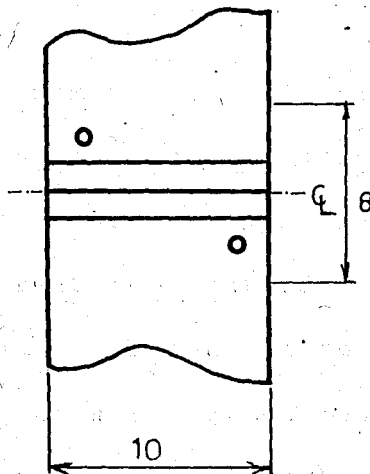
Fig. 2.8- Location of potential leads.

In actual specimens the crack front is always curved |20|. Crack advance is faster inside and slower outside which is a result of plane stress condition on the surface of the specimen and plane strain condition inside the specimen. With this in mind it can be said that this offset location will give results which reflect an average of the curved crack front (Fig. 2.9). To check this on real specimen the specimen has been removed from the machine of testing and heat

tinted. This way the crack boundary could be seen after comp-
letion of the fracture upon reloading (See. Section 3.2).
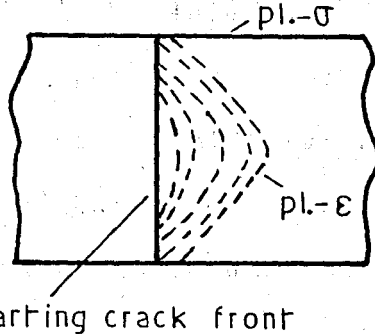
Fig. 2.9- Schematic drawing of successive positions of crack
fronts in a predominantly square fracture.

In order to minimize thermal emf dissimilar metal
junctions should be avoided when possible. These will affect
the results especially when the specimen and the measuring
devices are at different temperatures. In this study, since
the experiments were carried out at room temperature usage of
dissimilar metals in connecting the test piece to electrical
devices did not limit the useful working range of the volt-
meter.

The wire connections between current source and the
specimen and between voltmeter and the specimen are extremely
important. These might contribute large errors or save the
whole experiment. So, for current source-specimen junction
copper wires of 6 mm^2 cross section have been chosen. This
way the resistance and voltage drop on the wire have been
minimized. Shortness of the wire is also important because of
the possible heating effects. In connecting the wires to the
specimen copper tags have been used.

For voltmeter-specimen junction co-axial cable has been preferred. Thus obtained shielding avoided any noise. Since the measured voltage outputs were of the order of 10^2-10^3 µV any deviations due to noise would mislead the results. Here tags of phosphor-bronze have been used. Again because of noise danger the co-axial cable has been held as short as possible.

One last precaution was earthing. The application of a single good earth is essential to prevent errors from noise as mentioned in literature|1|.

Setting everything ready (Fig. 2.10) experimentation started which followed the same way as was proceeded with paper models, namely every specimen with different a/W ratio was connected to the system and after giving the current corresponding voltage was measured and recorded.
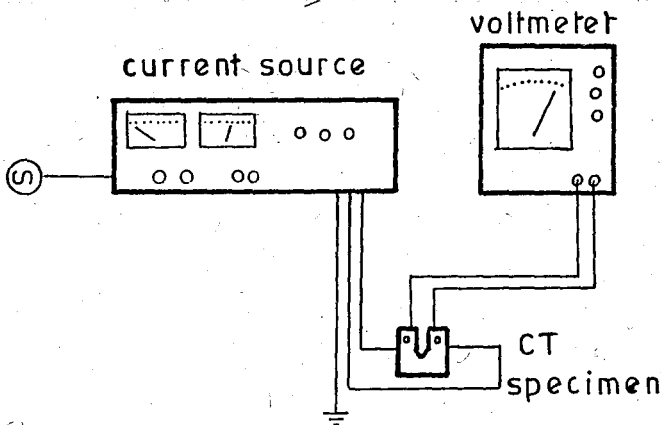
Fig. 2.10- Schematic drawing of the experimental set-up

To decide on the value of current to be applied several data has been obtained. Reduction of data was based on the range of the voltmeter, since any current starting with 10 A going up to 17 A gave measurable results. At the end the highest current value applied, 17 A has been preferred. Taking the non-dimensionalized voltage outputs (V_a/V_{a_o}) and plotting them against a/W ratio showed quite good fit with that of the paper analogs (Fig. 2.11).

So, it may be concluded that the calibration curve for compact tension is found by paper analogs and the results have been verified by using real metallic specimens.
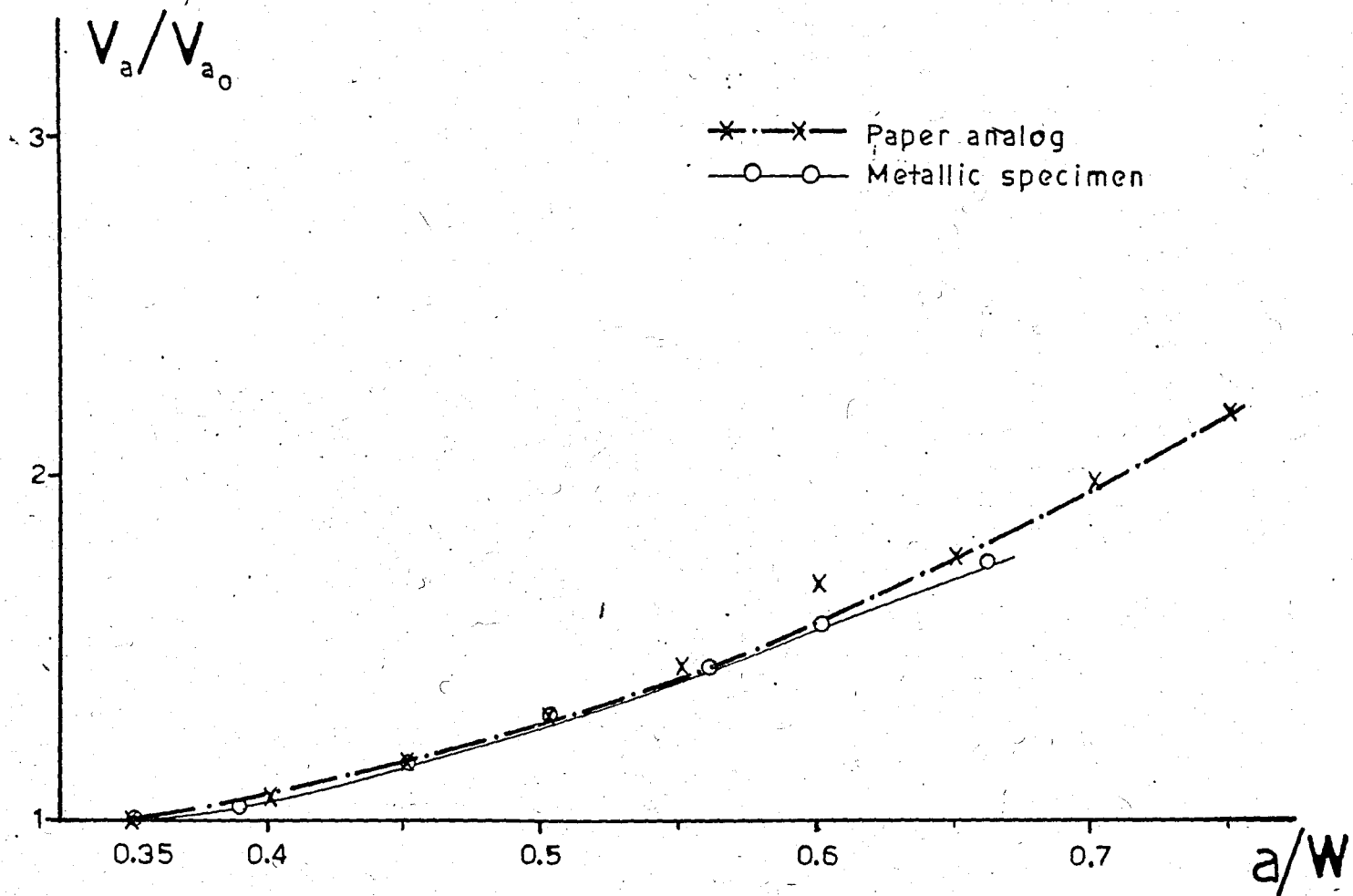
Fig. 2.11- Calibration curves for compact tension specimen obtained in two
different ways.

CHAPTER 3. TESTING ON MTS

After the calibration curve for compact tension speci-
men has been obtained by paper analogs and the result verified
by metallic specimens the latter have been tested on MTS 812-
a closed loop, servo hydraulic testing system with a maximum
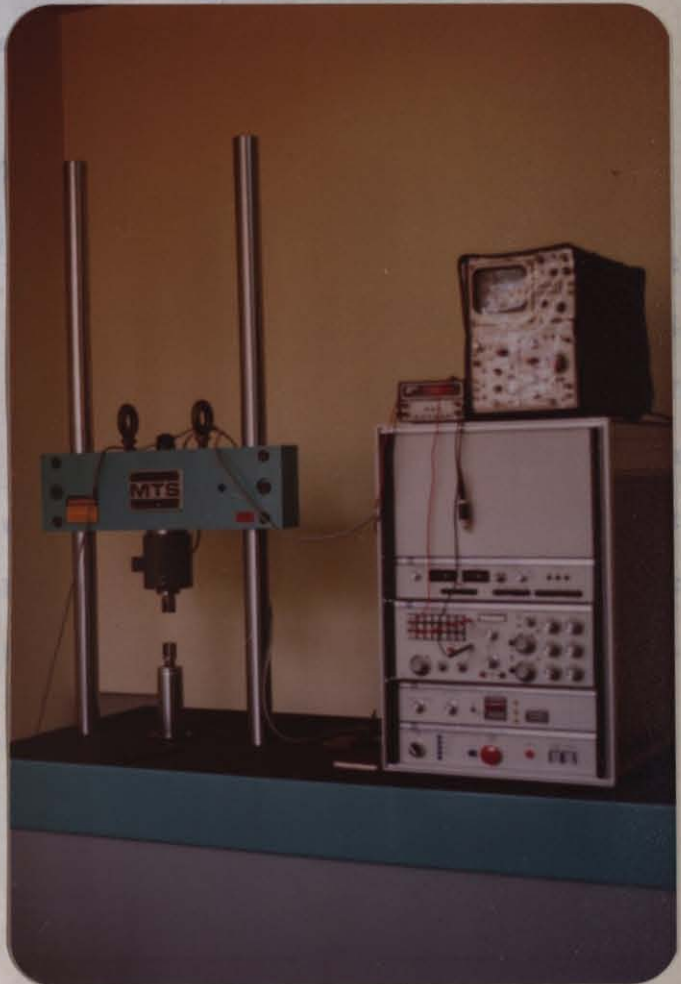load capacity of 10 tons (Fig. 3.1).

Fig. 3.1- A photo showing
MTS 812

First the specimens have been precracked in fatigue.
The conditions necessary for a sharp, flat crack normal to
the specimen edge are completely met by MTS (namely, load
distribution be symmetrical with relation to the notch in
planes normal to the thickness direction and the maximum
value of the stress intensity in the fatigue cycle be known
with an error of not more than 5 %|18|).

The equipment used in applying the electrical potential
technique at this stage was the same as in Section 2.6.1. The
only difference in measuring voltages was that the specimens
had to be fully isolated. For this TEFLON film and phenolic
fiber -to coat the pins of the grips- have been used.

3.1. FATIGUE CRACK INITIATION

To initiate fatigue crack specimens have been mounted
to the testing device. In order to accelerate the initiation
the keyhole type crack starter notch is marked with a knife.
A total of 5 specimens have been precracked in tension-tension
fatigue. To determine whether fatigue cracking was completed
within wanted limits observation of the traces of the crack on
the side surfaces of the specimens was sufficient (Fig. 3.2).

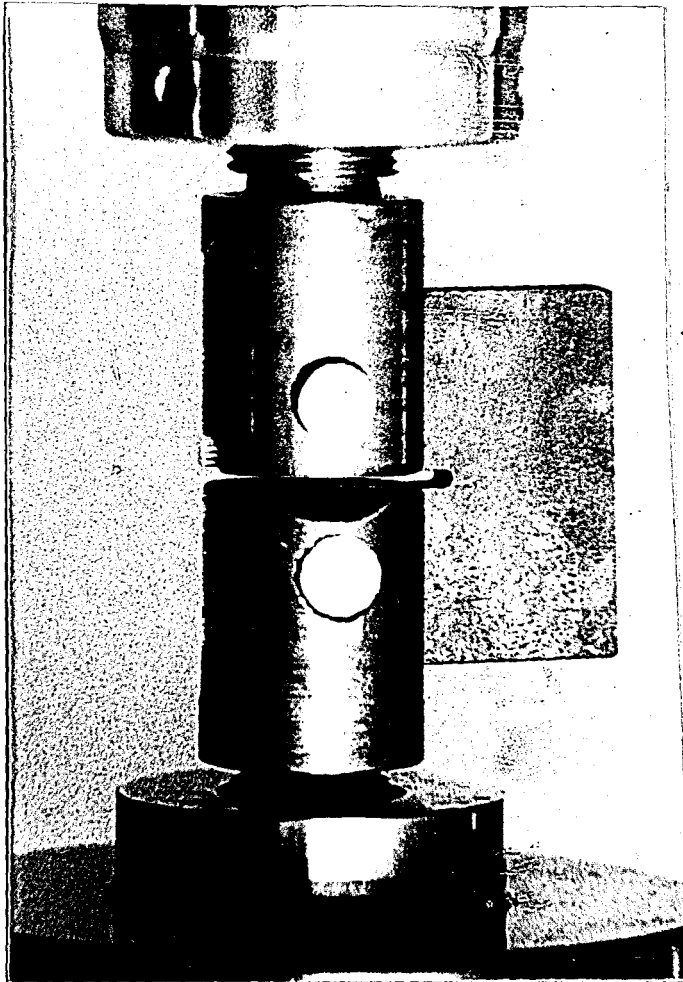Fig. 3.2- Specimen No. 6 in mounted position. The
crack propagating at the notch can be
easily seen.

The relevant data of crack initiation is summarized in

Table 3.1. As an addition the nominal stress at the notch

root* has been calculated and listed.

---

* Stress at the notch root is given by:

$$\sigma = \frac{P}{A} + \frac{Mc}{I} = \frac{P}{BW} \frac{2(2 + \frac{a}{W})}{(1-\frac{a}{W})^2}$$

TABLE 3.1

Crack Initiation Data

Specimen Number	a/W	ρ(mm)	ΔP(kg)	N_i	$\Delta\sigma_{notch}$ (kg/mm^2)
4	0.35	1.25	÷1400	100 000	–
5	0.39		100–1000	18 580	24.6
6	0.45		100– 800	22 870	24.1
A	0.56		100– 500	142 000	22.5
B	0.60		100– 575	12 250	32.8

The frequency -although not critical in this case- is held at about 5 Hz.

In specimen B while precracking reversed plastic deformation is observed.

3.2. MEASUREMENT OF CRACK LENGTHS

Once fatigue precracking was completed crack lengths of 5 specimens have been measured in two different ways. First, electrical potential technique was applied. The specimen with 4 leads (2 for current input, 2 for voltage output) is placed into insulated grips. A current of 17 A is given and each specimen is loaded to the maximum load given in Table 3.1, so the corresponding voltage could be read. The application of maximum load aimed a complete separation of crack surfaces. To check if any change in potential is observable with decrasing load, applied loads are decreased up to

0. The only specimen yielding a change of about 2% in voltage output was number B, which was plastically deformed in precracking (See Section 3.1).

After measurement of the voltages the specimens have been reloaded at maximum load and small wedges have been placed in crack starter envelope, such that during heat tinting crack surfaces could be completely oxidized. Following this, specimens have been put into furnace at about 300°C for approximately 5 hours. Thus heat tinted specimens were pulled to fracture, resulting fracture surfaces photographed and the crack length measured with a Mitutoyo pocket comparator.

Only for specimen number 6 it was possible to propagate the fatigue crack such that another data could be taken.

The fracture surfaces of specimens 5, A and B are seen in Fig. 3.3 while those of 6 are shown in Fig. 3.4. Specimen number 4 was not pulled to fracture at the moment, such that a comparison concerning it is missing. The dark surfaces in both photos represent the oxidized surfaces whereas the bright ones are fracture surfaces. The fatigue cracks -also oxidized- are more or less curved, maximum depth being in the middle as expected (See, Section 2.6.1). In Fig. 3.4 heat tinted fatigue crack is dark and curved while the propagated fatigue crack boundary is light and fracture surface bright. The bright section within the propagating fatigue crack is probably due to a crack arrest.

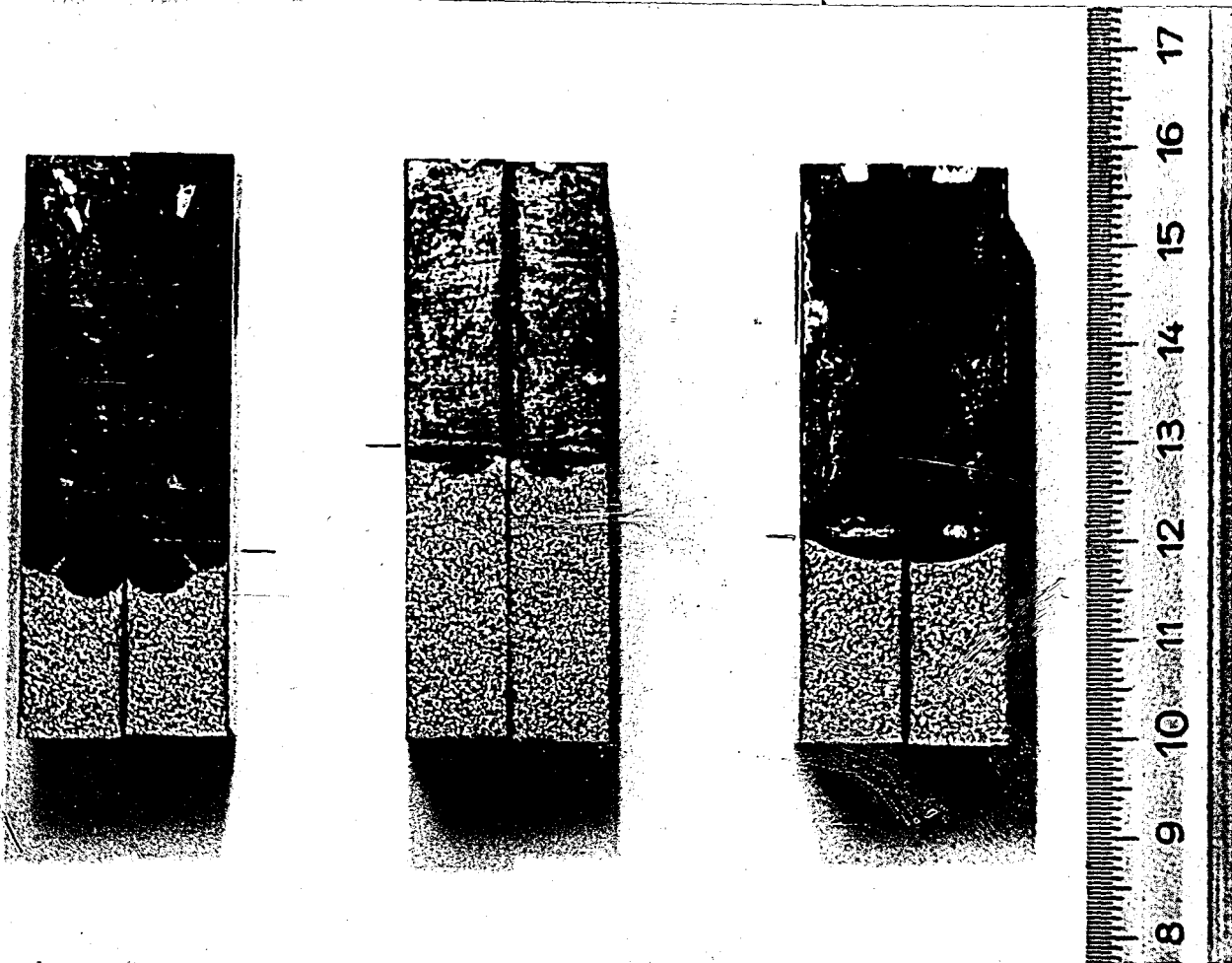Fig. 3.3- Fracture surfaces of specimens no B,
5 and A.

All the data summarizing the results of the two
different methods of measurement and including a comparison
is given in Table 3.2.

For specimen 5,6 and A percentage errors of 1-2 %
exist. For specimen B because plastic deformation has been
observed data from electrical potential method is varying
from 30.88 to 31.30 mm, thus resulting errors from 0.4-1.8 %.

TABLE 3.2

Results and Comparison of Two Different Methods of Measuring
Crack Length

Specimen No	P(kg)	$V_a(\mu V)$	V_a/V_{a_o} [1]	$\dfrac{a_{cal.}}{W}$ [2]	a_e (mm) [3]	a_m (mm) [4]	% Error
4	1400	640	1.20	0.465	21.855		)
5	1000	610	1.14	0.431	20.26	20.45	0.9
6	800	685	1.28	0.490	23.03	23.53	2.1
6[5]	900	880⁻	1.64	0.616	28.95		12.8
	125	870	1.63	0.612	28.76	}33.21	13.4
	45	860	1.61	0.610	28.67		13.7
A	500	860⁻	1.60	0.605	28.435	28.09	-1.2
B	575	980⁻	1.83	0.666	31.30		0.4
	470	975	1.82	0.662	31.11		1.05
	150	970	1.81	0.658	30.93	}31.44	1.6
	105	960	1.80	0.657	30.88		1.8

1) V_{a_o} = 535 µV

2) a/W obtained from calibration curve

3) Crack length found out from electrical potential method

4) Crack length measured from photographs

5) After fatigue crack has been propagated
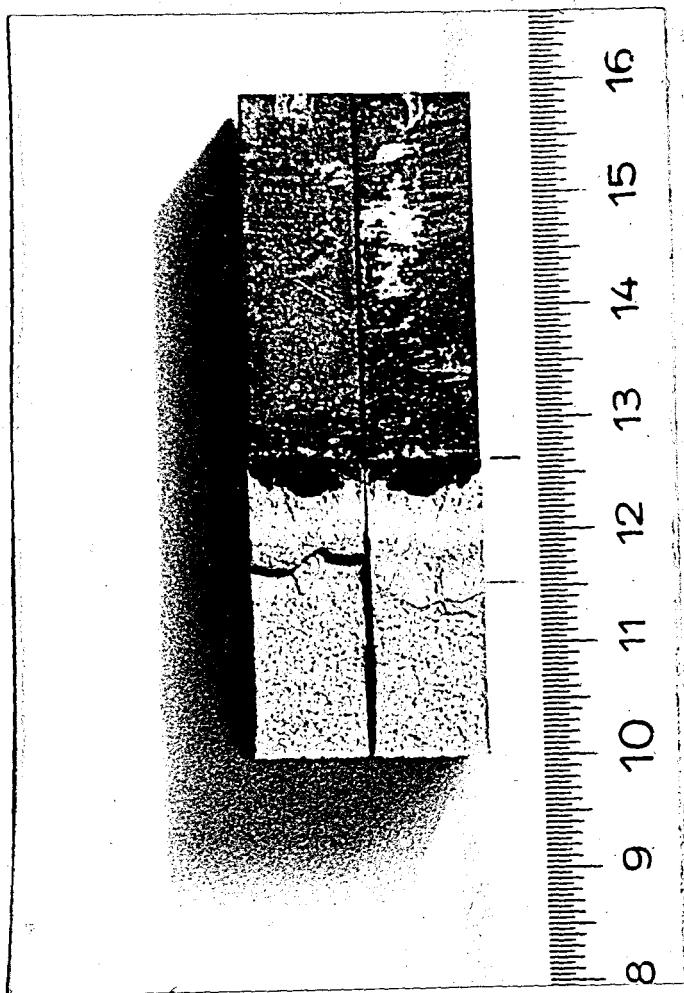
Fig. 3.4- Fracture surfaces of specimen no. 6

Again for specimen 6 after fatigue crack propagation variation of voltage with changing load is observed. The resulting errors are between 12.8-13.7 %. Since the results of electrical potential method are all less than the value obtained from direct measurement it can be said that the bright section (See Fig. 3.4), which was thought to be the result of a crack arrest, is responsible for that. This section has the same surface as the fracture surfaces. Then, it may be said that it was not torn completely while fatigue

crack was propagating, such that electrical current could
pass through resulting in a smaller voltage output.

As to conclude, the results obtained from electrical
potential method measurements are in error of 1-2 % when
compared with direct measurement. But since the data is
restricted with three (5, 6 and A) specimens* only it is hard
to judge the reliability of the technique. One thing that
must be said about this method is that it is very practical
for measuring crach lengths once all the requirements are met
completely.

---

* Specimen B, because of plastic deformation and specimen 6
  after fatigue crack propagation, because of not completely
  torn fracture surface are not taken into account at this
  stage.

CHAPTER 4
THE DISADVANTAGE OF THE METHOD:
PLASTIC DEFORMATION AT THE CRACK TIP

The major disadvantage of electrical potential method is the effect of the plastic deformation on the resistivity of the specimen. It is known generally that any impurity in lattice structure as well as any defect or plastic deformation of the material will contribute to the resistivity[21]. Although some experimental results have been found to relate some of the defects in lattice structures to increases in resistivity, a successful theoretical interpretation is still missing. So, unfortunately no quantitative predictions can be made based on theory. In experimental fracture analysis, 3[15, 20] to 4[22] zones in load-potential curves are discriminated, one of them being zone of plastic deformation.

One proposed method is estimation of the extent of the crack tip plasticity using finite element analysis based on the load applied to the specimen under test[16]. Knowing the change in electrical resistance with deformation additional

variation in potential can be determined. These compared with the elastic solutions will make a separation of the potential changes due to crack extension and due to crack tip plasticity possible. Thus the method will be improved in detecting crack initiation and monitoring crack growth.

This proposal actually fails in that it requires knowing the change in electrical resistance with deformation.

In this study only specimen B showed some plastic deformation and its effect on the method can be observed. Since the formation of a plastic zone at the crack tip when working with real materials -whether ductile or brittle- is unavoidable, the application of the electrical potential method could be restricted, to cases where the size of plastic deformation is known to be small/negligible.

REFERENCES

|1| R.O.Ritchie, Crack Growth Monitoring: Some Considerations
on the Electrical Potential Method, Report, Department
of Metallurgy and Materials Science, University of
Cambridge, Jan. 1972.

|2| R.O.Ritchie, G.G.Garrett and J.F.Knott, Crack Growth
Monitoring: Optimization of the Electrical Potential
Technique Using an Analog Method, Int. Journal of Frac-
ture Mechanics, Vol.7, 1971, pp.462-467.

|3| A.Trost, Ermittlung von Rissen und Messung der Risstiefen
in metallischen Werkstoffen durch electrische Spannugs-
messung, Metallwirtschaft, Vol.23, 1944, pp.308-309.

|4| G.Gille, Die Potentialsondenmethode und ihre Anwendung
auf die zerstörungsfreie Prüfung grosser Werkstücke,
Maschinenschaden, Vol.29, 1956, pp.123-127.

|5| W.J.Barnett and A.R.Troiano, J. of Metals, Vol.9, 1957,
p.486.

|6| E.A.Steigerwald and G.L.Hanna, Initiation of Slow Crack
Propagation in High Strength Materials, Proceedings,
ASTM, Vol.62, 1962, pp.885-913.

|7| H.H.Johnson, Calibrating the Electrical Potential Method
for Studying Slow Crack Growth, Materials Research and
Standards, Vol.5, 1965, pp.442-445.

|8| A.A.Anctil, E.B.Kula and E.DiCesare, Electric Potential
Technique for Determining Slow Crack Growth, Proceedings,
ASTM, Vol.63, 1963, pp.799-808.

|9| Che-Yu Li and R.P.Wei, Calibrating the Electrical Poten-
tial Method for Studying Slow Crack Growth, Materials
Research and Standards. Vol.6, 1966, pp.392-394.

|10| D.M.Gilbey and S.Pearson, Measurement of the Length of a
Central Crack or Edge Crack in a Sheet of Metal by an
Electrical Resistance Method, Technical Report 66402,
Royal Aircraft Establishment, 1966.

|11| P.McIntyre and A.H.Priest, Bisra Open Report MG/54/71,
1971.

|12| G.Clark and J.F.Knott, Measurement of Fatigue Cracks in
Notched Specimens by Means of Theoretical Electrical
Potential Calibrations, Journal of the Mechanics and
Physics of Solids, Vol.23, 1975, pp.265-276.

|13| R.Müllner, U.Rüdiger and K.E.Hagedorn, Ermittlung von
Ermüdungsrisslängen in Bruchmechanikproben mit dem
Potentialsondenverfahren, Archiv für das Eisenhütten-
wesens,Vol.48, 1977, pp.501-504.

|14| K.E.Hagedorn and U.Rüdiger, Ermittlung von Ermüdungs-
risslängen in Bruchmechanikproben aus Stahl RSt 37-2 mit
dem Potentialsondenverfahren, Archiv für das Eisenhüt-
tenwesens, Vol.46, 1975, pp.283-286.

|15| B.Marandet, G.Labbè, J.Pinard and M.Truchon, Detection de l'amorcage et suivi de la propagation d'une fissure par variation du potentiel electrique en regime alternatif, IRSID Rep.Re. 549, 1978.

|16| R.O.Ritchie and K.J.Bathe, On the Calibration of the Electric Potential Technique for Monitoring Crack Growth Using Finite Element Methods, International Journal of Fracture, Vol.15, 1979, pp.47-55.

|17| G.H.Aronson and R.O.Ritchie, Optimization of the Electrical Potential Technique for Crack Growth Monitoring in Compact Test Pieces Using Finite Element Analysis, Journal of Testing and Evaluating, Vol.7, 1979, pp.208-215.

|18| Standard Test Method for Plane-Strain Fracture Toughness of Metallic Materials, ASTM Designation: E 399-74, 1974.

|19| H.S.Pearson and P.F.Packman, Fracture Testing Guidelines for Engineers, Fracture Prevention and Control, Proceedings, ASMM/Metalworking Technology Series, no:3, Ed. by David W.Hoeppner, 1974.

|20| J.E.Srawley and F.B.William, Jr., Fracture Toughness Testing Methods, ASTM STP:381, 1975, pp.133-198.

|21| I.Kovacs and L.Zsoldos, Dislocations and Plastic Deformation, Oxford, New York, Pergamon Press, 1973, pp.246 - 249.

|22| V.Bachmann and D.Munz, Unusual Potential Drop During the Application of the Electrical Potential Method in a Fracture Mechanics Test, Journal of Testing and Evaluating, Vol.4, 1976, pp.252-260.